Proceedings of the
Annual Stability Conference
Structural Stability Research Council
Baltimore, Maryland, April 10-13, 2018

Modeling Out-of-Flatness and Residual Stresses in Steel Plate Girders

Mahdi Asadnia[1], W. M. Kim Roddis[2]

Abstract
As the girder buckling strength depends on residual stresses and initial out-of-flatness, these need to be modeled when quantifying their effects. Zhang in 2007 used single plate imperfection patterns for web out-of-flatness for I-shaped plate girders. Actual girder out-of-flatness patterns include imperfections in all plate elements. This study uses a whole body out-of-flatness pattern compatible with the total body first buckling mode shape (Sadovsky 1978). An imperfection free girder Finite Element Model (FEM) is analyzed in ANSYS Software for Elastic Buckling, using the same loading and boundary conditions as the desired final imperfect steel plate girder, to generate the first buckling mode shape. The nodes of the imperfection free steel plate girder are displaced into the buckled shape and this distorted geometry is then used for non-linear analysis. Yield stress at the welded intersection of flange and web is the basis for residual stress distributions, generated using Heat Analysis in ANSYS to obtain temperature distributions. Lateral bracing is used to prevent global lateral torsional buckling so local buckling controls the flexural moment at onset of yielding. This approach allows a study of the effect of different magnitudes of geometrical imperfection for a set of girder cross-sections for I-shaped plate girders. The flexural moment at onset of yielding for various scales of the buckled shape are normalized by the imperfection free steel plate girder moment, giving a measure of the effect of the size of out-of-flatness on the performance of the girder. The results of FEA show dependency of first yield moment to web slenderness ratios and out-of-flatness in I-shaped plate girders. There is the critical web slenderness ratio of 124 for unstiffened I-shaped girders which causes the most strength reduction for positive moments and drastic strength reduction for larger slenderness for negative moment. No reverse behavior or critical web slenderness was observed in stiffened I-shaped girders for 1D, 2D, and 3D transverse stiffener spacings. The out-of-flatness tolerance was relaxed when it was strength wise possible. The proposed strength-based web out-of-flatness criteria are provided for I-shaped plate girders. Adopting total body first buckling mode shape as out-of-flatness pattern resulted in more conservative web tolerance than Zhang's proposed web tolerance for unstiffened I-shaped girders at positive moments.

1. Introduction
Reasonable tolerances for steel plate out-of-flatness are required during fabrication and construction of built-up structural members. For American highway bridges out-of-flatness

[1] PhD Student, The George Washington University, <masadnia@gwumail.gwu.edu>
[2] Professor, The George Washington University, <roddis@email.gwu.edu>

tolerances are currently set for some elements, but the engineering basis for these is not clear (Herman 2001). This study determines the girder strength reduction associated with out-of-flatness for I-shaped girder webs and flanges. Finite Element Analysis (FEA) is used to construct flexural strength reduction curves for girders with various out-of-flatness magnitudes, covering a range of girder cross-sections and spans. This study examines steel girders rather than composite girders. Before setting of the concrete deck and formation of composite action, the steel girder alone must support all the steel, concrete, and falsework weight. This is a critical situation caused by compressive stresses resulting in local buckling and instability. These compressive stresses exist in the upper flange at the middle of simply supported span and in the lower flange at the interior pier of continuous I-shaped plate girders.

2. Finite Element Modeling

The goal for this finite element modeling and analysis is to study a whole body out-of-flatness pattern and residual stress effects on flexural design strength of I-shaped plate girders. This work closely follows that done by Zhang in 2007, except that work used out-of-flatness in one plate and 50 ksi steel. The yielding moment for I-shaped girders including initial out-of-flatness, $M_{y\Delta}$, is different from the theoretical yielding moment strength defined by linear elastic beam theory which is calculated as $M_y = F_y S_x$. $M_{y\Delta}$ refers to this FEA determined first yield moment (Zhang 2007). Web slenderness ratios and out-of-flatness magnitudes are the two most significant parameters in this study affecting flexural strength for I-shaped plate girders. These two parameters are varied in I-shaped girders for single span and continuous two-span models to obtain their effects on first yield and ultimate flexural strength. The large deformation analysis was used to include the effect of out-of-flatness. The Arc-Length method was used to capture the post-collapse phase to clearly distinguish the ultimate strength point. The Newton-Raphson method was used to capture the behavior up to ultimate flexural moment. The first yield moment was then extracted. Stiffened and unstiffened I-shaped plate girders are modeled. Web slenderness ratios and out-of-flatness magnitudes are the two most significant parameters in this study affecting strength of I-shaped girders. These two parameters are varied in the FEMs so their effects on first yield moment can be quantified. A set of dimensions spanning normal sizes is chosen for I-shaped section. Each I-shaped girder is modeled and analyzed for a range of different out-of-flatness magnitudes. Since the governing behavior of concern in this study is local buckling, straight I-shaped girders are used to evaluate out-of-flatness tolerance. The following sections describe various aspects of modeling including the pattern and inclusion of residual stress and out-of-flatness.

2.1 Residual Stress Pattern and Modeling

The uneven cooling of the metallic structures during and after welding, thermal and mechanical mill procedures create permanent self-balancing stresses in the steel called residual stresses. Fig. 1 shows the residual stress pattern used in the finite element steel I-shaped plate models. The residual stress is assumed to be the yield stress at the welds connecting the web and each flange and to be negligible at the four flange edges. The modeling of residual stresses in the FEMs used trial and error to find the heat boundary conditions that would generate the desired pattern shown in Fig. 1. This procedure was followed for each case using a set of ANSYS Software’s Finite Element Heat Analyses. Fig. 2 depicts the temperature boundary conditions. These values included temperatures at the upper flange edges and upper and lower web and flange intersections. These quantities are labeled A, B, and D in Fig. 2. Fig. 2 also shows the convection properties of upper and lower flange and web surfaces. These properties have been labeled C, E, and F in Fig. 2. The thermal property of steel used is listed in Table 1. The stresses at the flange and web intersections were checked for yielding stresses. If the self-balancing stress distributions had not created the desired residual stress pattern, as depicted in Fig. 1, the temperature boundary conditions in the model would be changed until the desired stress distributions were obtained. Once the correct temperature boundary conditions for a particular I-shaped girder and out-of-flatness were found, the associated strain distribution in the structure was imported into the applicable Static Analysis girder model. This imported strain domain generated a stress domain equivalent to that of the residual stresses.

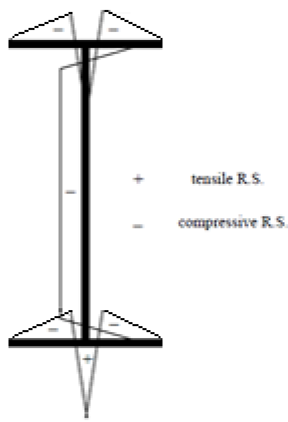

Figure 1: Residual Stress Pattern Used in the FE Steel I-Shaped Plate Girders.
The Positive Peak Values Are Yielding Stress at Tension at the Welding Locations.

According to Zhang, the residual stresses cause negligible added out-of-flatness in the models. This statement was also confirmed in this research. Fig. 3 shows the final residual stresses at the cross section of a typical stiffened I-shaped girder FEM made of grade 50 steel.

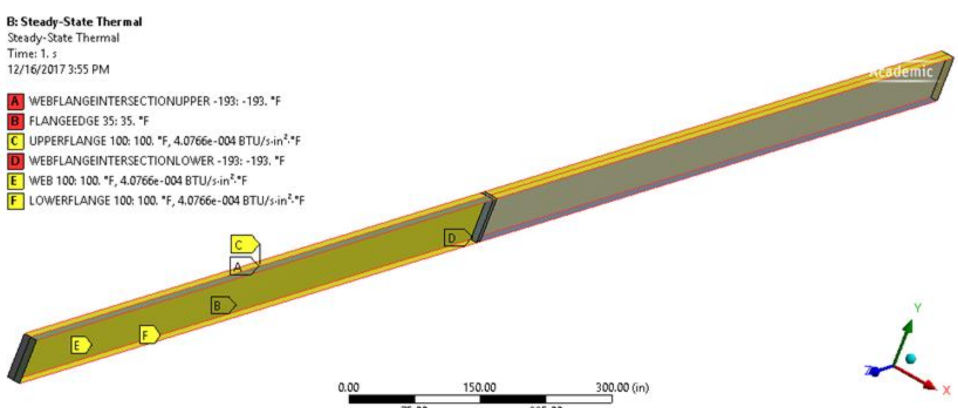

Figure 2: Finite Element Thermal Analysis Boundary Conditions for an Unstiffened Continuous Two-Span I-Shaped Girder Creating Yielding Strains at the Intersection of Flange and Web.

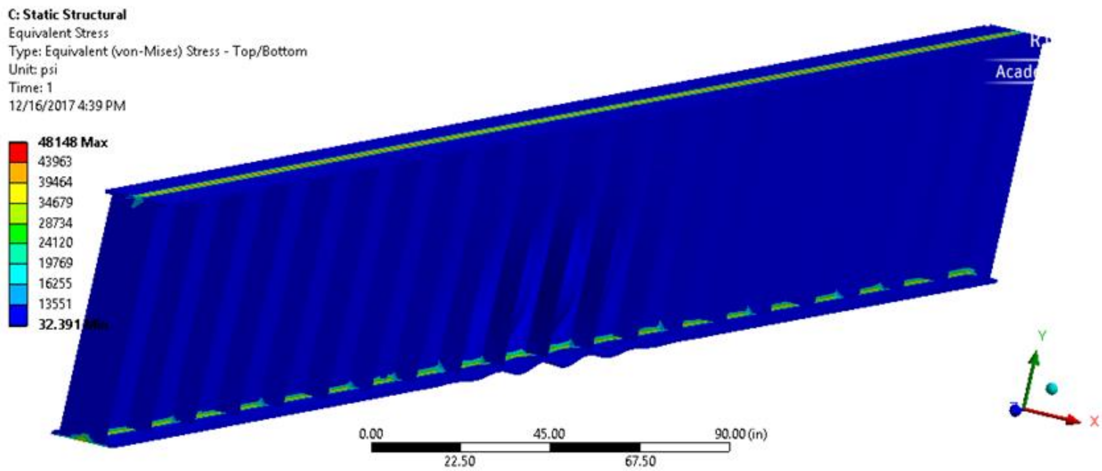

Figure 3: Residual Stresses of a Grade 50 Tub Girder Showing Yielding Stresses at the Intersections of Flanges and Webs.

2.2 Out-of-Flatness Pattern and Modeling

Different approaches have been used for modeling out-of-flatness in the FEMs of plate girders. There is not a unique pattern of out-of-flatness in actual plate girders, as these are of a random nature (Korol et al. 1984). A field survey of built steel plate girders has shown that actual out-of-flatness of steel girders are both in web and flanges together (Zhang 2007). In 1978 Sadovsky proved that the out-of-flatness pattern compatible with the first buckling mode shape would result in the lowest theoretical buckling strength for steel plates. This study uses a whole body out-of-flatness pattern compatible with the total body first buckling mode shape. These buckling shapes were obtained using linear buckling analysis. Fig. 4 depicts the first buckling mode shape of a typical unstiffened I-shaped plate girder at positive flexural moment location. Existence of web and flange out-of-flatness are clear in Fig. 4. Fig. 5 shows the first buckling mode shape for a typical stiffened plate girder with intermediate stiffeners installed at 2D distances, which D the section height.

Eight web out-of-flatness magnitudes were used to generate various out-of-flatness for I-shaped plate girders:

$$\Delta_o = \frac{b_f}{100{,}000}, \frac{b_f}{500}, \frac{b_f}{200}, \frac{b_f}{150}, \frac{b_f}{100}, \frac{b_f}{50} \text{ and } \frac{b_f}{10}. \tag{1}$$

For each I-shaped plate girder, the first yield moment for $\Delta_o = \frac{b_f}{100{,}000}$ was considered as the yielding moment for a perfect girder free from all out-of-flatness. It was necessary to consider a non-zero out-of-flatness for the perfect girder because zero out-of-flatness resulted in divergence of the geometric non-linear analysis. This perfect girder first yield flexural moment was used to normalize the results for other out-of-flatness (Zhang 2007).

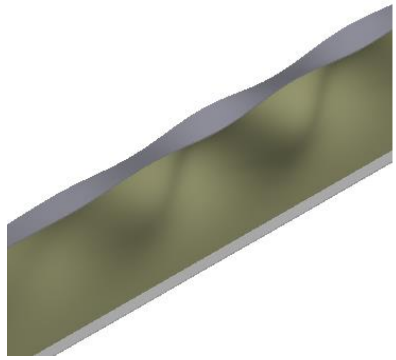

Figure 4: Whole Cross Section First Buckling Mode Shape for a Typical Unstiffened I-Shaped Plate Girder. Adopted from ANSYS Software.

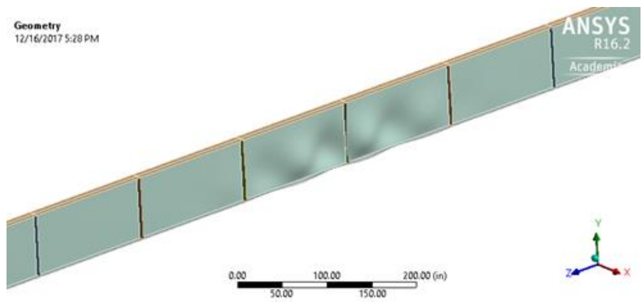

Figure 5: Whole Cross Section First Buckling Mode Shape for a Typical Stiffened I-Shaped Plate Girder 2D Stiffener Spacing. Adopted from ANSYS Software.

2.3 Steel Constitutive Models and Properties

Fig. 6 illustrates typical strain-stress curves for different standard steels used in construction

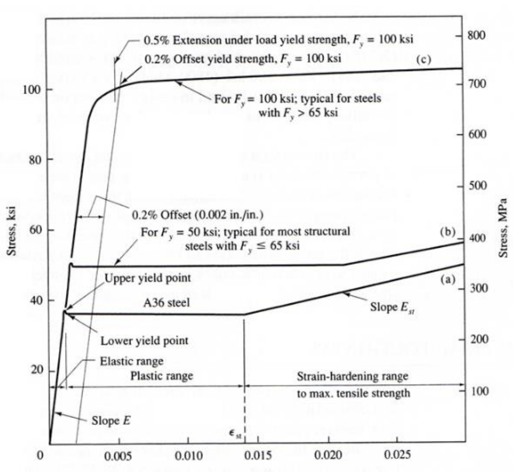

Figure 6: Typical Steel Strain-Stress Curve. Adopted from: (Salmon et al 2008).

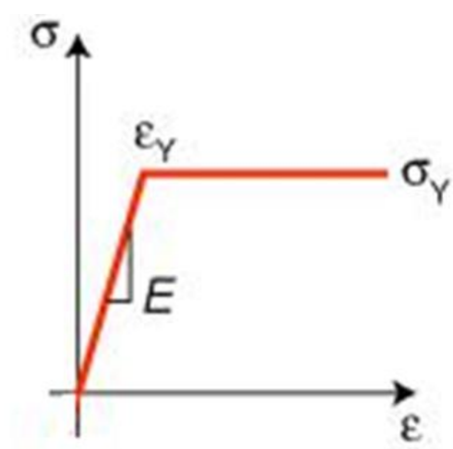

Figure 7: Elastic-Perfectly Plastic Constitutive Model.

(Salmon et. al 2008). The graphs include grade 36, 50 and 100 steels. The yielding strains for these three steel grades are 0.0012, 0.0017 and 0.0034 accordingly. The hardening strain at which the hardening behavior of steel is started is about 0.02. It is 16, 11 and 5 times the yielding strain of grade 36, 50 and 100 steel accordingly (Salmon et. al 2008). Fig. 7 shows the Elastic-Perfectly Plastic constitutive model for the steel in I-shape plate steel bridges in this study. The assumption of no-hardening behavior at first yield moment limit state was confirmed at the end of this study considering the magnitudes of total strain at onset of yielding which were much smaller than hardening strains.

Table 1: Material Properties for Finite Element Analysis Models.

Young's Modulus of Elasticity	29,000 ksi
Poisson's Ratio	0.3
Yield Stress	50 ksi, 100 ksi
Tangent Modulus (after yielding)	0
Secant Coefficient of Thermal Expansion	6.5E-06 in./in./F

2.4 Element Type and Meshing

In finite element solution of differential equations, each equation is solved for each individual element. The proper choice of elements is required to capture and model the intended behavior of the structure. There are many pre-defined element types in ANSYS Software which are chosen based on the best match for the situation. In this process the prevailing force, dominant structural behavior, and relative geometrical dimensions are some of the factors considered in choosing proper element types. Academic ANSYS v16.2 and v15 software used SHELL 181 to construct the plate component of plate girder FEMs. Per ANSYS manual, SHELL181 is appropriate for analyzing thin to moderately-thick shell structures and it is a four-node element with six degrees of freedom at each node: translations in the x, y, and z directions, and rotations about the x, y, and z axes. SHELL181 was well-suited for linear, large rotation, and/or large strain nonlinear applications and both full and reduced integration schemes are supported in the element domain (ANSYS 2013). SHELL181 includes the effects of transverse shear. The dependency of the strength, deflection and out-of-flatness shape to the number of elements that build the model was evaluated. This dependency determined the required number of elements in the FEMs to achieve necessary precision in results at optimal time.

Fig. 8 shows a sketch of the 4-node SHELL181. Each side of the shell element has a linear shape function as it includes two nodes. Fig. 9 illustrates the meshed geometry of a typical continuous I-shaped plate girder at the internal support. Fig. 10 shows the meshed geometry of a typical stiffened I-shaped plate girder. Bearing stiffeners are visible in Fig. 9 and Fig. 10 which resist concentrated forces. Fig. 11 illustrates meshed geometry for a typical imperfect unstiffened I-shaped plate girder. The total body out-of-flatness including upper flange and web geometrical imperfection are visible in Fig. 11.

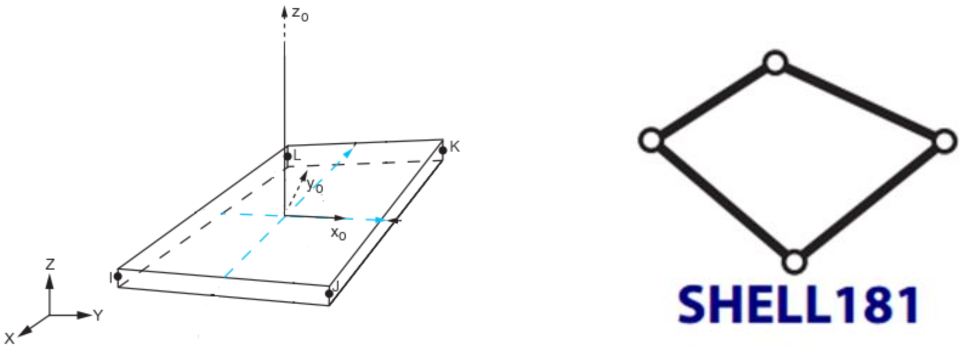

Figure 8: ANSYS Software 4-node Quadrilateral Shell Element (SHELL181).

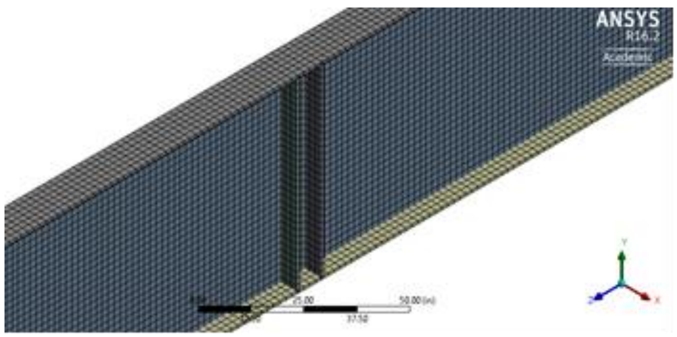

Figure 9: Meshed Continuous Unstiffened I-Shaped

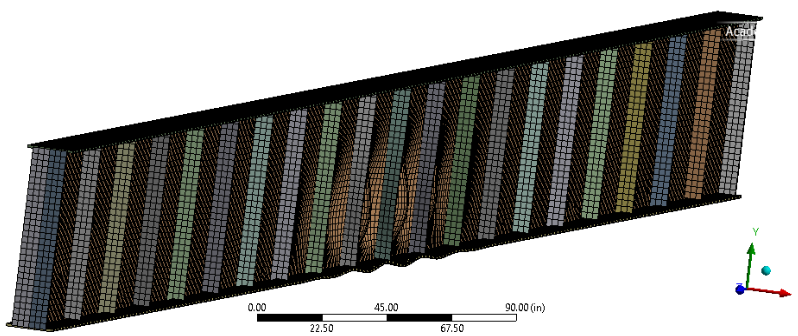

Figure 10: Meshed Stiffened I-Shaped Plate Girder Plate Girder.

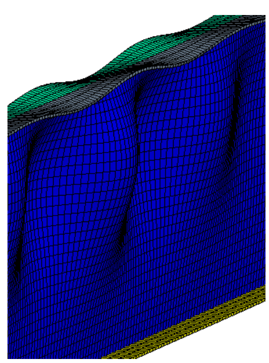

Figure 11: Meshed Geometry for an Imperfect Unstiffened I-Shaped Plate Girder.

2.5 Large Deformation and Large Strain Analysis

When the deformation in a structure increases to large magnitudes, the changing geometry due to this deformation can no longer be neglected. Obtaining the intended behavior of geometrically imperfect I-shaped girder under load requires consideration of changing geometry resulting from previous load steps in each new load step as the structure is loaded to the point of yielding. In this situation, the geometry is changed and updated at each load step to include the deformation as the new geometry. The Large Deflection option in Static Structural was turned on in ANSYS Software in this research to capture the secondary moments because of out-of-flatness.

2.6 I-Shaped Plate Girder Dimensions

The geometric configurations of the I-shaped plate girders were adopted directly from Zhang 2007. They were checked to comply with current design practice AASHTO/LRFD (2017). The upper and lower flanges of I-shaped plate girders were designed as compact to prevent local buckling of flanges. The following web slenderness were selected to cover most of non-compact web slender ranges and part of the web slender range, h_w/t_w= 90, 100, 112, 124, 137 and 150 (Zhang, 2007). Table 2 depicts unstiffened steel I-shaped plate girders simply supported finite element models analyzed and their specifications including flange width, flange thickness, section height, web thickness and steel yielding stress. Table 3 shows unstiffened steel I-shaped plate girders continuous two-span models analyzed and their specifications. These two tables also include the name of the models. Fig. 12 shows the cross sections and the dimensions of six I-shaped steel plate girders used in the finite element analysis of I-shaped steel plate girders and the span lengths adopted from Zhang. Fig. 12 include all cross-section dimensions used in stiffened, unstiffened, simply supported, and continuous span I-shaped plate girder.

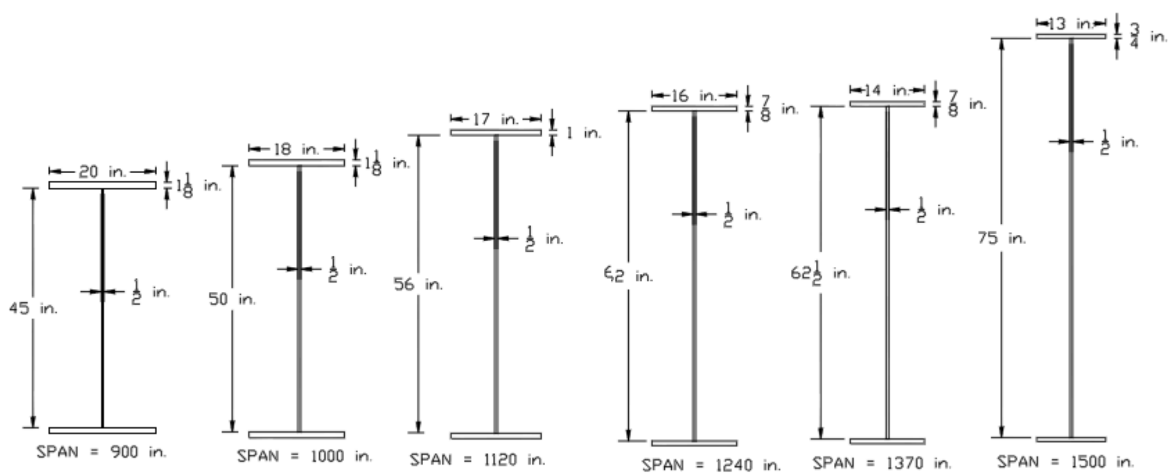

Figure 12: Dimensions Used in the Geometric Non-Linear FE Analysis of I-Shaped Steel Plate Girders. Adopted from (Zhang 2007).

All, except one of the I-shaped plate girders, were analyzed only for grade 50 steel. The same unstiffened I-shaped plate girder dimensions were used for stiffened plate girder having 1D, 2D, 3D, and 4D spacing, where D is depth of the plate girders. The stiffeners were designed to satisfy AASHTO requirements for minimum plate thickness (Zhang 2007). Table 4 shows the summary of stiffened I-shaped plate girders geometric designations.

Table 2: Summary of Unstiffened I-Shaped Plate Girders FEMs Simply Supported.

FEM Name	Span Length(in.)	Flange Width (in.)	Flange Thickness (in.)	Section Height (in.)	Web Thickness (in.)	Yielding Stress (ksi)
L900Bf20Tf1.125H45Tw0.5	900	20	1.125	45	0.5	50
L1000Bf18Tf1.125H50Tw0.5	1000	18	1.125	50	0.5	50
L1120Bf17Tf1H56Tw0.5	1120	17	1	56	0.5	50
L1240Bf16Tf0.88H62Tw0.5	1240	16	0.88	62	0.5	50
L1370Bf14Tf0.88H62.5Tw0.5	1370	14	0.88	62.5	0.5	50
L1500Bf13Tf0.75H75Tw0.5	1500	13	0.75	75	0.5	50

Table 3: Summary of Unstiffened I-Shaped Plate Girders FEMs Continuous, Two-Span.

FEM Name	Span Length(in.)	Flange Width (in.)	Flange Thickness (in.)	Section Height (in.)	Web Thickness (in.)	Yielding Stress (ksi)
50KsiL900Bf20Tf1.125H45Tw0.5	900	20	1.125	45	0.5	50
50KsiL1000Bf18Tf1.125H50Tw0.5	1000	18	1.125	50	0.5	50
50KsiL1120Bf17Tf1H56Tw0.5	1120	17	1	56	0.5	50
50KsiL1240Bf16Tf0.88H62Tw0.5	1240	16	0.88	62	0.5	50
100KsiL1240Bf11Tf0.88H62Tw0.5	1240	11	0.88	62	0.5	100
50KsiL1370Bf13Tf0.875H68.5Tw0.5	1370	14	0.88	62.5	0.5	50
50KsiL1500Bf13Tf0.75H75Tw0.5	1500	13	0.75	75	0.5	50

Table 4: Geometric Parameter Designation of the FEA Stiffened Plate Girder. Adopted from (Zhang 2007).

Geometric Parameters	**Values**
Web Slenderness (D/t)	90 100 112 124 137 150
Web Out-of-flatness (Δ_o/D)	1/1000 1/500 1/200 1/150 1/100 1/50
Stiffener Spacing (d_o/D)	1 2 3 4

2.7 Static Structural Boundary Condition

The setup of boundary conditions is an essential part of FEA to achieve a credible solution while solving for its stability. Some of steel bridge I-shaped plate girder models in this study were simply supported. Some of the FEMs were continuous two span I-shaped steel plate girders. For the simply supported girders, one end was supported by pin support and the other end was supported by roller support. Fig. 13 illustrates the definition of a pin support at one end of the girder. The pin support is defined as the highlighted edge with no translational degree of freedom in any direction. This method of defining the pin support prevented creation of stress concentration and early yielding or collapse at the end supports. The goal of this research was to concentrate on local stability of the girders. This dictated making lateral bracing lengths shorter than restrictive unbraced length for formation of plastic flexural moment. This conservative bracing length assured prevention of global Lateral Torsional Buckling (LTB), which was not a topic of interest in this study. Fig. 14 depicts the static structural boundary condition for a typical unstiffened I-shaped simply supported girder analyzed for positive flexural moment at the middle. The boundary conditions are labeled B, D, and E in Fig. 14. The boundary conditions considered were: lateral support restraining I-shaped girder from global lateral torsional buckling, left pinned support, and right roller support. The loadings included uniform downward upper flange load and imported strains causing residual stresses. The loadings are labeled as A and C in Fig. 14.

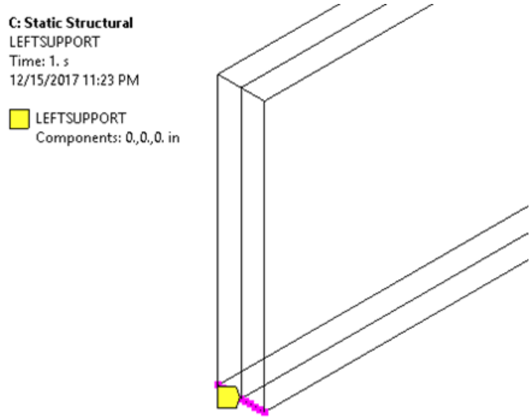

Figure 13: Definition of Simple Support in a FEM.

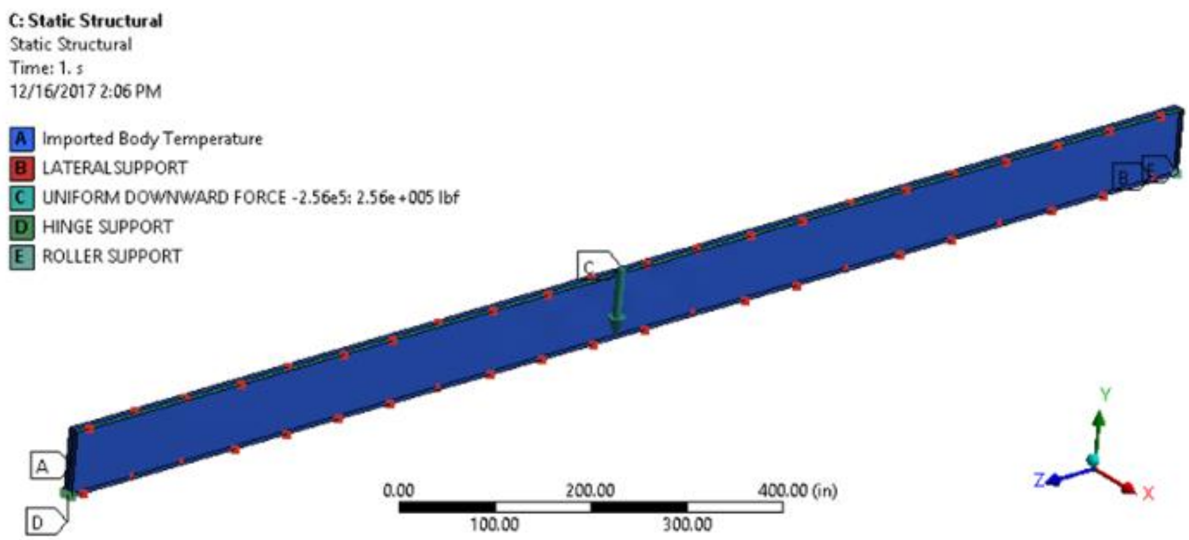

Figure 14: FEA Model for an Unstiffened I-Shaped Including Loading and Boundary Conditions.

These flexural moment measurements were performed 1" before the interior support for the negative moment of continuous two-span girders. The 1" distance was considered to avoid dealing with concentrated stresses at bearing stiffeners and its corners.

3. Finite Element Analyses Results

The discussions of the calculated parameters in the FEMs are provided in following sections.

3.1 I-Shaped Plate Girder Unstiffened Positive Moment

Fig. 15 and Fig. 16 shows the normalized ultimate positive flexural moment at the middle of two simply supported I-shaped plate girders. The post failure results were obtained using the Arc-Length method. The peak of the load vs. deflection shows the actual ultimate strength of the girder. Reviewing Fig. 15 and 16 discloses that for each girder with the same dimensions, larger out-of-flatness has caused earlier collapse, or greater reductions of ultimate strength. Most cases showed that the ultimate strength reduction was less than 15% of $M_{u\_D/100,000}$, the ultimate strength of the perfect girder. Fig. 17 displays the results of all analyses together for unstiffened I-shaped steel plate girders. The x-axis is the web slenderness ratio and the y-axis is the normalized ultimate strength, $M_u/M_{u\_D/100,000}$. This figure clearly shows that for the same out-of-flatness the ultimate strength reduces up to a web slenderness ratio of 124 and then it increases slightly for higher web slenderness values. This observation approximately agrees with that of Rangelov (Rangelov 1992) and Sadovsky (Sadovsky 1996). They found the maximum reduction happens at the web slenderness ratio of 137 and 139 respectively. They only considered the web out-of-flatness, but in this modelling the out-of-flatness in the flanges were also considered as well compatible with the first buckling mode shape. Fig. 18 depicts the web slenderness ratio versus normalized moment at onset of yielding obtained by Newton-Raphson method. The curves in Fig. 18 shows similar trends to those in Fig. 17 for ultimate strength. The trend between the strength reduction effect of web out-of-flatness and web slenderness reversed at the critical web slenderness of $\frac{D}{t}$=124. It is obvious that out-of-flatness caused a more significant reduction in the yielding strength of the girders than they did for ultimate strength. For example, the maximum reduction of yielding strength for the $\frac{D}{100}$ out-of-flatness was more than 15% and that caused by the $\frac{D}{50}$ out-of-flatness was greater than 20%. Evidently, the plate out-of-flatness is more structurally detrimental in terms of causing earlier onset of yielding in the plate girders. The out-of-flatness in plates induce larger out-of-plane deformation of the webs at low load level and therefore contribute to earlier onset of the yielding in plate girders. The stress distribution deviates from the typical linear stress distribution across the web depth because of the loss of the stiffness in the upper web.

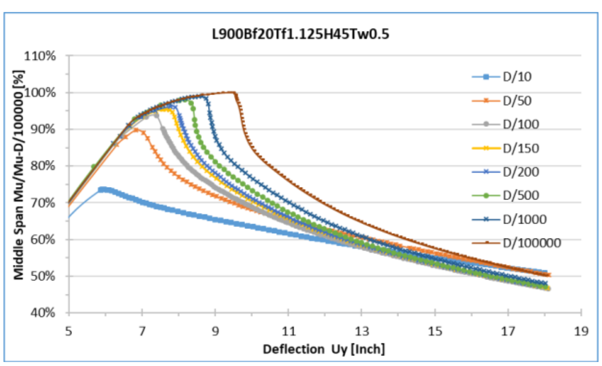

Figure 15: FEA Results of Load-Displacement Response for Unstiffened I-Shaped Steel Plate Girders ($\frac{D}{t_w}$=90).

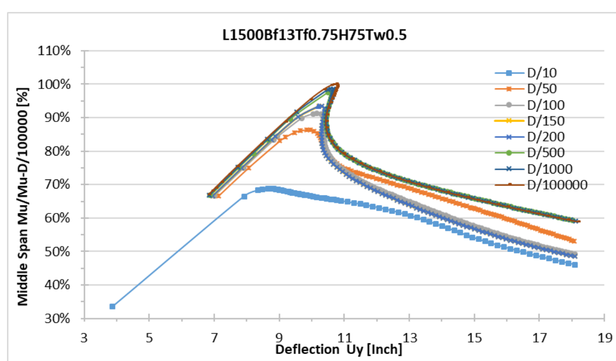

Figure 16: FEA Results of Load-Displacement Response for Unstiffened I-Shaped Steel Plate Girders ($\frac{D}{t_w}$=150).

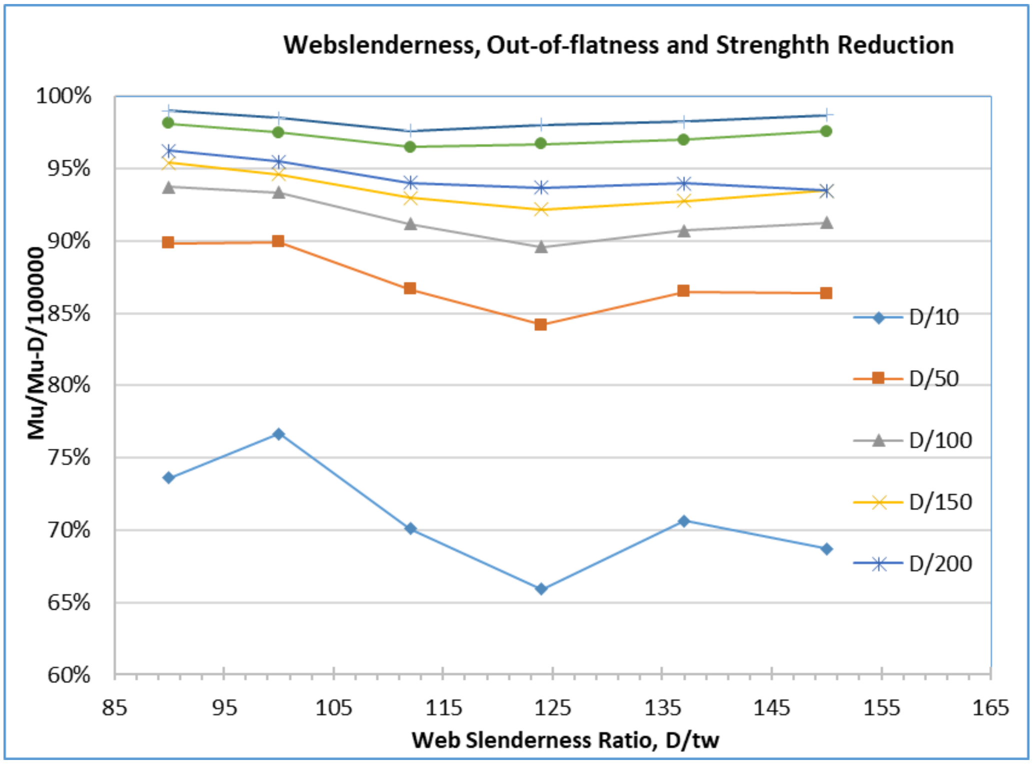

Figure 17: Normalized Ultimate Strength ($M_u/M_{u\_D/100,000}$) vs. Web Slenderness ($\frac{D}{t}$) for Unstiffened I-Shaped Steel Plate Girders.

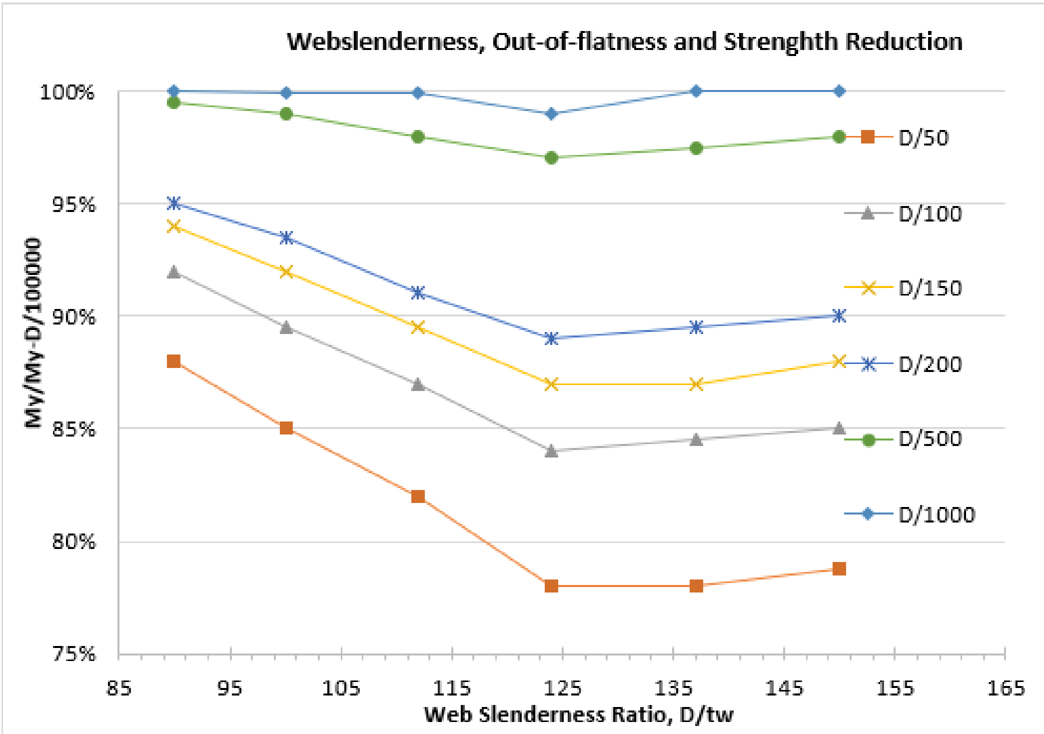

Figure 18: Normalized Yielding Strength ($M_{y\Delta}/M_{y\Delta\_D/100000}$) vs. Web Slenderness ($\frac{D}{t}$) for Unstiffened I-Shaped Steel Plate Girders.

Inclusions of flange out-of-flatness caused a change in the critical web slenderness ratio. As the flanges had proportional out-of-flatness in comparison to the perfect flange assumption of Zhang, the twisting and buckling of the flanges initiated easily at the smaller web slenderness ratio. The flange out-of-flatness were compatible with first buckling mode shape. The amount of strength reduction was more in models having web and flange out-of-flatness in comparison to the models having only web out-of-flatness with perfect flanges. Assumption of out-of-flatness pattern compatible with first buckling mode shape caused both out-of-flatness flange and web which were more compatible with reality. The deformation shape and von Mises stresses during the collapse of a typical unstiffened I-shaped girder presented in Fig. 19 as an example to demonstrate the collapse mechanism.

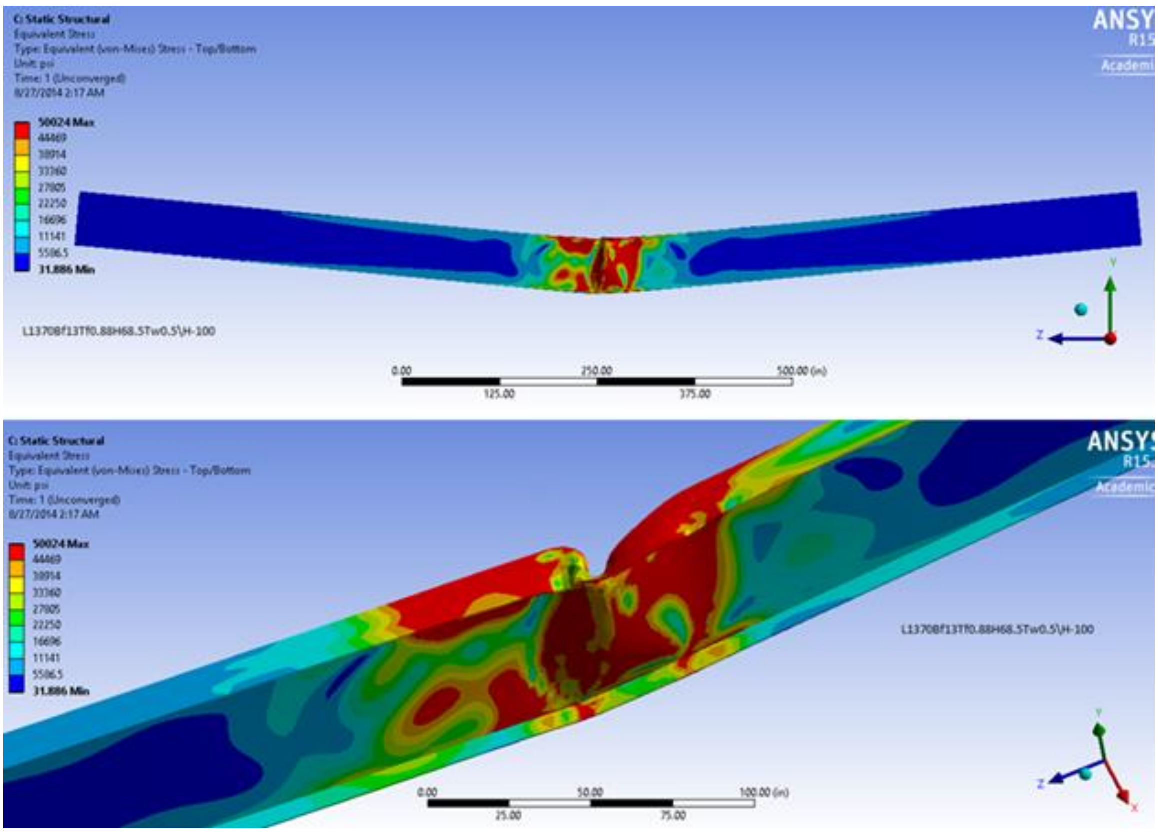

Figure 19: Collapse Mechanism and Equivalent Stress (von-Mises) for an Unstiffened I-Shaped Grade 50 Steel Plate. Adopted from ANSYS Software

3.2 I-Shaped Plate Girder Stiffened Positive Moment

The unstiffened I-shaped plate girder models which were modeled previously were modified to have transverse stiffener. The designs of the transverse stiffeners were per AASHTO LRFD Specifications (AASHTO LRFD 2017). The stiffener spacing used in the models were 1D, 2D, 3D and 4D. To comply with AASHTO requirement, the stiffeners were not connected to the tensile flange and a gap was provided. The initial imperfect geometries are compatible with the first buckling mode shape and they include flange and web out-of-flatness. The flexural moment at the middle span was monitored. The monitored section at the middle span was moved slightly to exclude stiffeners and their local yielding effect. The normalized ultimate strength of all stiffened girder model with 1D spacing were obtained from the load-displacement curves and plotted in Fig. 20. The x-axis is the web slenderness ratio and the y-axis are the normalized ultimate strength, $M_u/M_{u\_D/100000}$. No trend reversal behavior was observed for the stiffened I-shaped girders. The normalized ultimate strength reduces as web slenderness increases. The normalized first yield moment,$M_{y\Delta}$, for stiffened I-shaped plate girders and different stiffener spacings are plotted in Fig. 21, 22, and 23. The first yield moment for each girder model was nondimensionalized by that corresponding to the perfect girder model,$M_{y\Delta\ D/1000}$. These graphs show larger web out-of-flatness cause more yielding strength reductions in stiffened plate girders. The reversal behavior for the critical web slenderness happened only for the 4D stiffener spacing. The large 4D stiffener spacing causes the I-shaped steel girder to act like unstiffened I-shaped plate girder. Fig. 24 shows total deformation and Fig. 25 depicts equivalent von-Mises stresses in FEA of stiffened I-shaped plate girders.

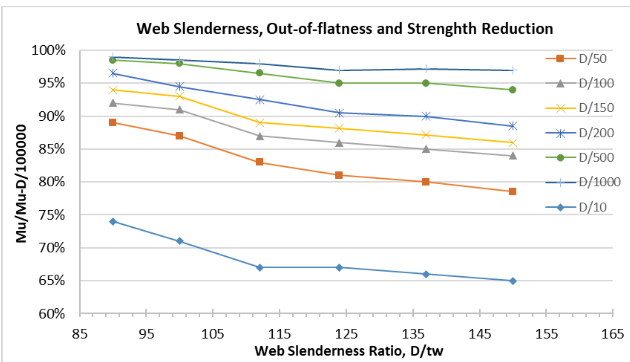

Figure 20: Normalized Ultimate Strength ($M_u/M_{u\_D/100000}$) vs. Web Slenderness ($\frac{D}{t}$) for Stiffened I-Shaped Plate Girder with 1D Spacing.

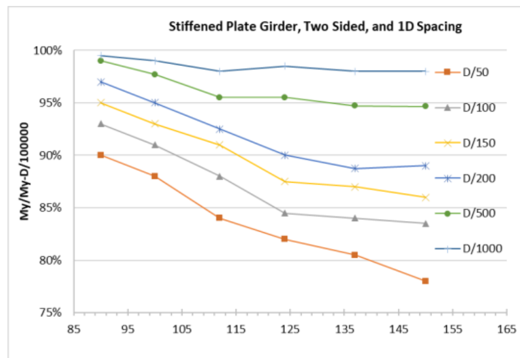

Figure 21: Normalized Yielding Strength ($M_{y\Delta}/M_{y\Delta\_\ D/100000}$) vs. Web Slenderness ($\frac{D}{t}$) for Stiffened I-Shaped Plate Girder with 1D Spacing.

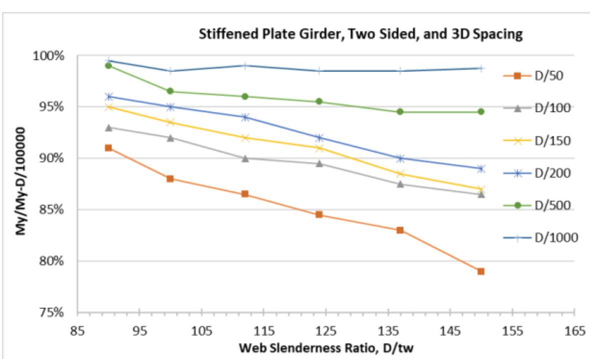

Figure 22: Normalized Yielding Strength ($M_{y\Delta}/M_{y\Delta\_\ D/100000}$) vs. Web Slenderness ($\frac{D}{t}$) for Stiffened I-Shaped Plate Girder with 3D Spacing.

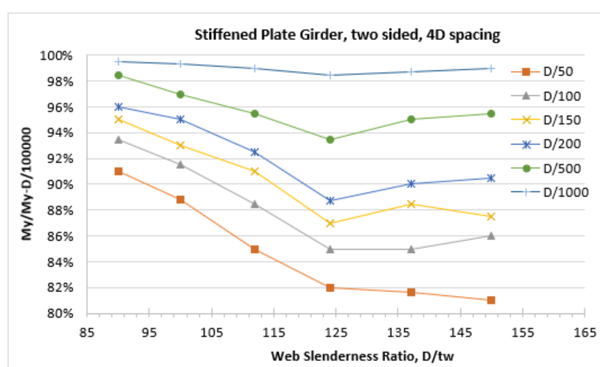

Figure 23: Normalized Yielding Strength ($M_{y\Delta}/M_{y\Delta\_\ D/100000}$) vs. Web Slenderness ($\frac{D}{t}$) for Stiffened I-Shaped Plate Girder with 4D Spacing.

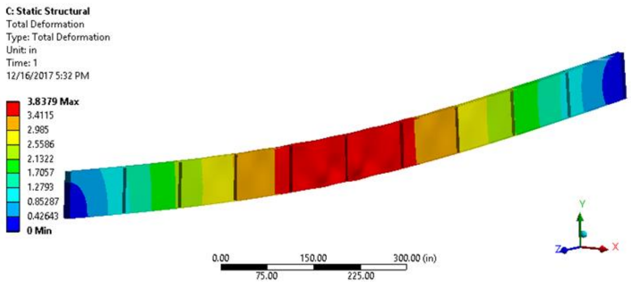

Figure 24: Total Deformation of Stiffened I-Shaped Grade 50 Steel Span=1500”, b_f=13”, t_f=0.75”, D=75”, t_w=0.5”, 2D Spacing and Out-of-Flatness of $\frac{D}{10}$.

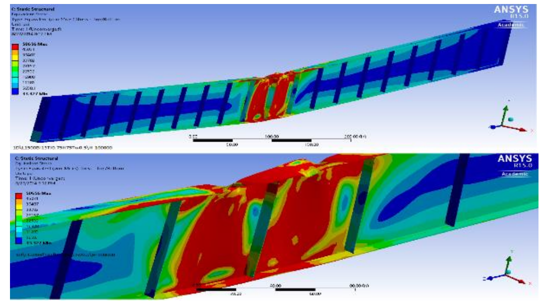

Figure 25: Equivalent (von-Mises) Stresses of FEA Model for a Stiffened Plate Girder after Collapse $(1\times \text{D Spacing})$.

3.3 I-Shaped Plate Girder Unstiffened Negative Moment

Fig. 26 and Fig. 27 show the result of FEA for two-span continuous unstiffened I-shaped plate girders. The negative moment at the internal pier at onset of yielding was monitored for various I-shaped plate girders. Fig. 28 displays normalized yielding strength versus web slenderness of

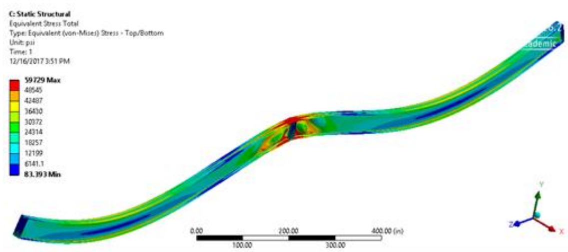

Figure 26: von-Mises Stress of a Two-Span Unstiffened I-Shaped Grade 50 Steel Span=2*900”, b_f=20”, t_f=1.125”, H=45”, t_w=0.5” and Out-of-flatness of $\frac{H}{200}$.

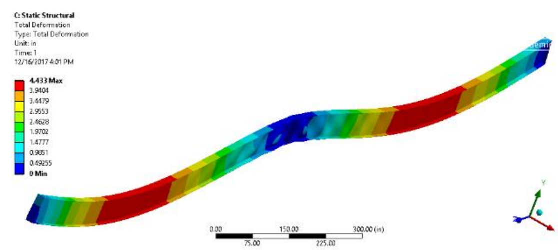

Figure 27: Total Deformation for a Two-Span Unstiffened Grade 50 Steel Span=2*1120”, b_f=17”, t_f=1”, H=56”, t_w=0.5” and Out-of-flatness of $\frac{H}{1000}$.

two-span girders having various out-of-flatness magnitudes, and different web slenderness. It was observed that the normalized strength at onset of yielding decreases gradually up to web slenderness of 124. The most yielding strength reduction up to this web slenderness is about 4% less than the perfect girder for out-of-flatness of $\frac{D}{50}$. The yielding strength reduction increases dramatically with higher rate for web slenderness larger than 124. The inclusion of geometrical flange out-of-flatness compatible with first buckling mode and its considerable magnitude for slenderer girder web can justify this behavior. For out-of-flatness of $\frac{D}{150}$ and web slenderness of 150 the strength reduction was about 20% of the perfect two-span girder. The web slenderness of 124 was a critical slenderness for the two-span unstiffened I-shaped steel girders. The results of analysis for two-span grade 100 steel showed slight deviation from the results of grade 50 steel girders. The normalized yielding strength reduction for web slenderness of 124 for grade 50 steel is 4%, but for grade 100 steel is 6%. Doubling yielding stress has caused 2% difference in the results. Up to web slenderness of 124 the strength reduction was mildly slow, but for web slenderness greater than 124 the strength reduced sharply. This behavior showed that the web slenderness between 124 and 150 for the negative moment was more vulnerable to the out-of-

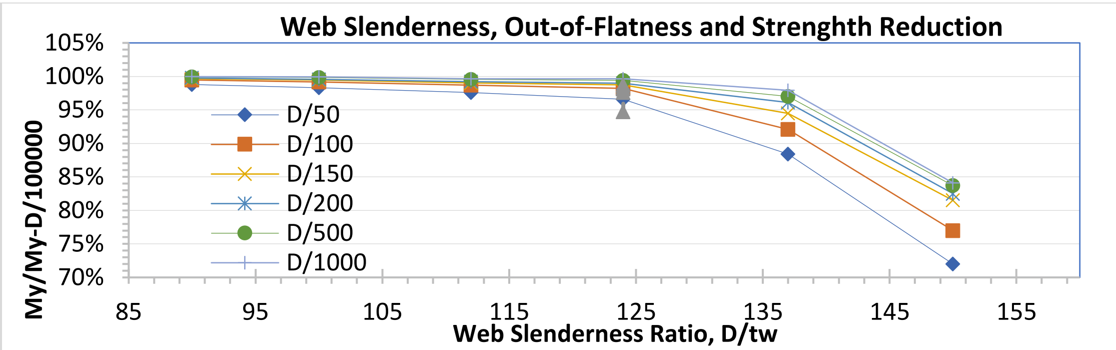

Figure 28: Normalized Yielding Strength ($M_{y\Delta}/M_{y\Delta\_D/100000}$) vs. Web Slenderness ($\frac{D}{t}$) for Continuous Two Span Unstiffened Plate Girders of Various Web Slenderness.

flatness. The out-of-flatness of $\frac{D}{150}$ caused maximum 19.5% strength reduction for web slenderness ratio of 150. The practical $\frac{D}{50}$ out-of-flatness caused maximum 3.4% strength reduction up to web slenderness ratio of 124.

4. Strength Based Web Out-of-Flatness Tolerances

4.1 I-Shaped Plate Girder Unstiffened Positive Moment

All flexural moment at onset of yielding for unstiffened I-shaped plate girder exposed to positive moment were obtained. Fig. 29 shows the result of normalized flexural moment at onset of yielding at the middle span of simply supported unstiffened I-shaped plate girders which were loaded uniformly in the vertical direction. The vertical axis shows the percent reduction in design strength and the horizontal axis shows the web slenderness ratios. It was observed that in all out-of-flatness magnitudes the yielding strength was decreasing with increase in the web slenderness ratio up to the web slenderness ratio of 124. For larger web slenderness ratios, the pattern was reversed and an increase in the yielding moment was observed. In other words, the web slenderness ratio of 124 was critical and caused the maximum strength reduction. It was observed that rate of strength increase after critical web slenderness ratio was smaller than slope of decreasingly downward line. A yielding strength reduction threshold was established based on the currently specified American Welding Society (AWS) Bridge Welding Code D1.5 specifications most restrictive web tolerance, $\frac{D}{150}$, for the critical web slenderness of 124. The 124-critical web slenderness ratio caused approximately 13% yielding strength reduction. The tolerance could be relaxed for girders with web slenderness smaller than $\frac{D}{t}$, =124. Linear regression analyses were conducted to determine the corresponding magnitudes of web out-of-flatness that could produce an equal amount, 13%, of yielding strength at web slenderness other than, $\frac{D}{t_w}$=124. Using the trend-line functions, one can input the threshold yielding strength, 87% corresponding to $\frac{D}{150}$ for critical web slenderness of 124 and solve the web slenderness at which the other out-of-flatness magnitudes would cause the same amount of yielding strength reduction. Considering the small reversal slope for web slenderness ratios of larger than 124 and the small range of web slenderness ratio between 124 and 150 in Fig. 29, conservatively the regression was not performed between 124 and 150 web slenderness ratios. Table 5 shows the steps in regression analysis for different out-of-flatness magnitudes in unstiffened I-shaped steel plate girders.

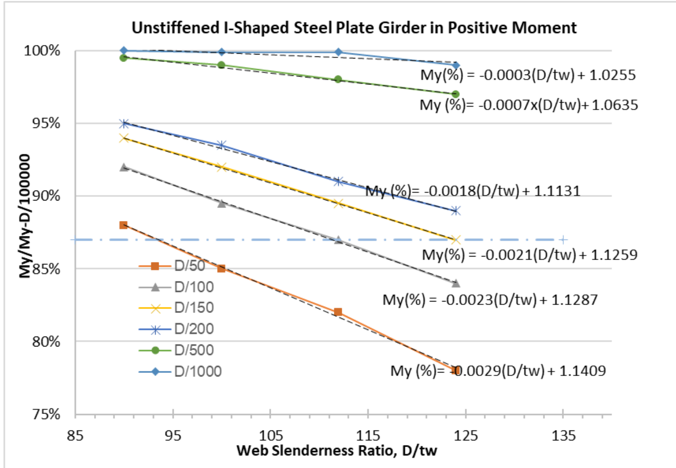

Figure 29: Regression Analysis for Unstiffened I-Shaped Steel Plate Girders in Positive Moments.

In Table 5, the trend-line formula for each out-of-flatness magnitude has been listed. For web out-of-flatness magnitudes of $\frac{D}{150}$ and larger, the corresponding web slenderness ratio was obtained based on 13% strength reduction at onset of yielding. The out-put $\frac{D}{t}$ in Table 5 is the web slenderness ratio that causes 13% strength reduction. All the trend lines have been graphed in Fig. 29. The green shaded data pairs in Table 5 were plotted in Fig. 30 to indicate the web out-of-flatness limits defined by the strength threshold for different web slenderness.

Table 5: Solutions for the Web Slenderness Having 13% Yielding Strength Reduction Caused by Different Amount of Web Out-of-flatness.

Web Out-of-Flatness Δ_0	**Input** $M_{y\Delta}/M_{y\Delta\ D/100000}$	**Trend-line Formula**	**Output** D/t
D/500	87.00%	**My (%)= -0.0007x(D/tw) + 1.0635**	276.4
D/200		**My (%)= -0.0018(D/tw) + 1.1131**	135.1
D/150		**My (%) = -0.0021(D/tw) + 1.1259**	121.9
D/100		**My (%) = -0.0023(D/tw) + 1.1287**	112.5
D/50		**My (%)= -0.0029(D/tw) + 1.1409**	93.4

In Fig. 30, the x-axis represents the web slenderness ratio, $\frac{D}{t_w}$, while the y-axis represents a plate tolerance coefficient, C, defined as $C = \frac{D}{\Delta_0}$. A trend-line was also drawn in Fig. 30 and corresponding formula $C = 3.4\,\frac{D}{t} - 270$ was obtained through linear regression analysis. It is worth of notice that obtained formula was limited to the web slenderness range $\frac{D}{t} < 124$ because the yielding strength reduction effects of the web out-of-flatness will reverse when $\frac{D}{t} > 124$. For I-Shaped plate girders with thicker plates, larger web out-of-flatness were allowed. However, large web out-of-flatness may also impair the aesthetic characteristics of the structure and thus needed to be prevented. Under such a concern, the proposed plate tolerance was limited to $\Delta_0 \leq \frac{D}{50}$ for cases with $\frac{D}{t} < 90$, which was the compact/noncompact slenderness limit for grade 50 steel (Zhang, 2007). For girders with slender webs ($\frac{D}{t} > 124$), slightly relaxed tolerance would be permissible from the viewpoint of strength reduction.

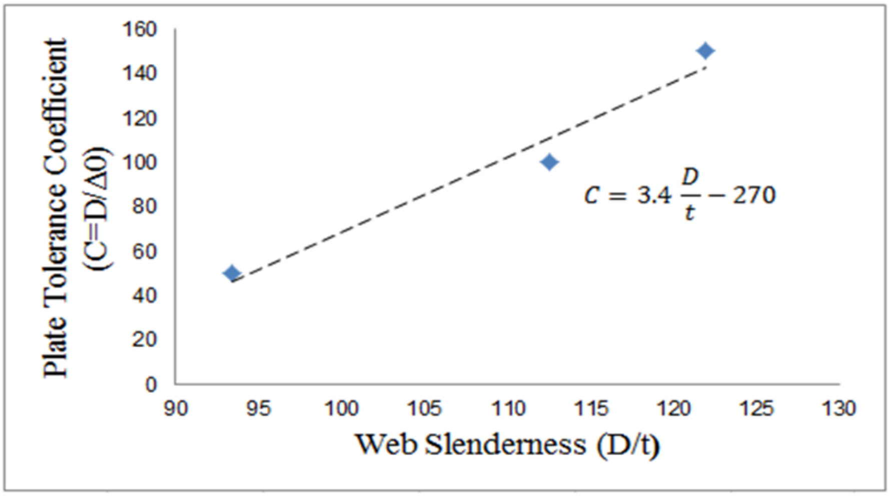

Figure 30: Strength-Based Plate Tolerance for the Web of Unstiffened I-Shaped Plate girder.

However, for slender webs, larger out-of-displacement of web plate can be resulted from excessive initial out-of-flatness, which may be detrimental to the fatigue life of the girders (Zhang, 2007). Therefore, the proposed plate tolerance was still limited by $\Delta_0 \leq \frac{D}{150}$ for cases with $\frac{D}{t} > 124$. A theoretically derived strength-based tolerance can be proposed based on the analysis described above. Based on the methodology offered by Zhang in 2007 the proposed unstiffened I-shaped plate girder web tolerance is expressed as $C = \frac{D}{\Delta_0}$ Where $C = 3.4\frac{D}{t} - 270$. Considering the above explanations, the coefficient C for the proposed plate tolerance can be expressed as: if $\frac{D}{t} \leq 90$ then C=50, if $90 < \frac{D}{t} < 124$ then $C = 3.4\frac{D}{t} - 270$, and if $\frac{D}{t} \geq 124$ then C=150. A comparison between the proposed, currently used and previously proposed web out-of-flatness tolerances is illustrated in Fig. 31. The current plate tolerance is based on AWS D1.5 for the geometrical web out-of-flatness tolerance of the unstiffened steel plate girders which is the constant value of $\frac{D}{150}$ for all the web slenderness ratios. The Zhang's criteria were obtained by assumption of only web out-of-flatness compatible with first buckling mode shape and perfect flanges with no out-of-flatness. The proposed plate tolerance is more relaxed than currently used plate tolerance. As the proportional flange, out-of-flatness has been also included in the models, the proposed plate tolerance is more conservative than Zhang's proposed plate tolerance for unstiffened I-shaped steel plate girders exposed to positive moments. Considering the out-of-flatness shape including both flanges and web out-of-flatness compatible with first buckling mode shape resulted in more conservative tolerance criteria in comparison to Zhang's proposed criteria. The obtained criteria were much more relaxed in comparison to current AWS D1.5 criteria.

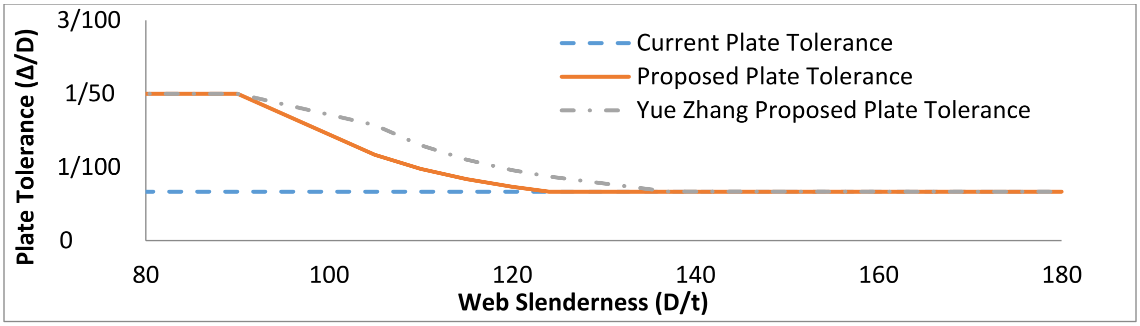

Figure 31: Comparison among Proposed, Current Plate Tolerance and Latest Proposed Tolerances for an Unstiffened I-Shaped Steel Plate Girder Web in Positive Moment.

4.2 I-Shaped Plate Girder Stiffened Positive Moment

Following similar regression analyses, web strength based out-of-flatness tolerances for interior two-sided stiffened I-shaped plate girder 1D, 2D, 3D and 4D spacing were obtained. Fig. 32 illustrates summary of all the obtained out-of-flatness criteria for four different double-sided stiffeners spacing. Although the out-of-flatness strength-based criteria for 1D, 2D and 3D stiffener spacing almost follow the same trend, there is a major pattern change for 4D stiffener spacing. This change of pattern can be described by dissipation of tension-field action for 4D spacing. Per AISC, "tension-field action is the post-buckling development of diagonal tensile stresses in slender plate-girder web panels and compressive forces in the transverse stiffeners that border those panels". The long distance of the transverse stiffeners for 4D deprives the stiffened I-shaped plate girder from formation of the tension-field action and the lack of diagonal tension-field omits the truss behavior in the I-shaped steel plate girder and its nature of behavior. This result is consistent with general idea that larger than 3D stiffener spacing is not helpful in creating the tension-field action.

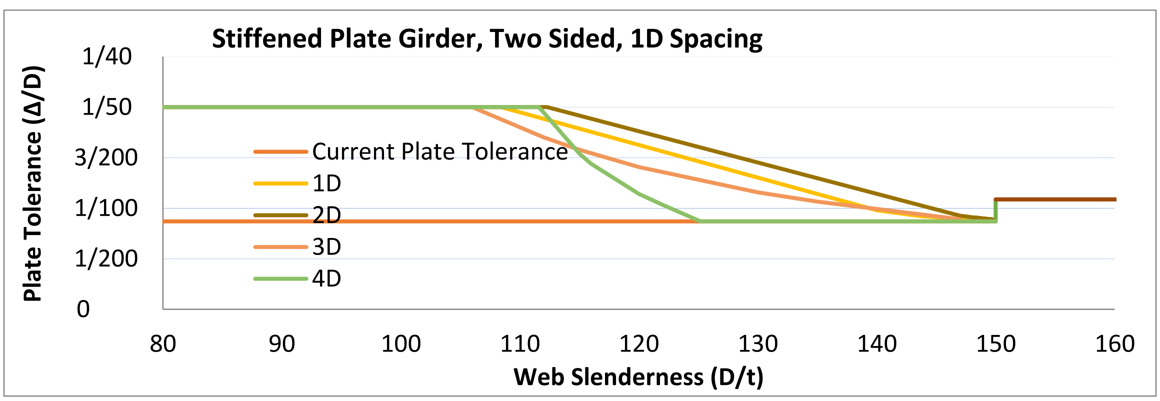

Figure 32: Interior Two-Sided Stiffened I-Shaped Plate Girder 1D, 2D, 3D and 4D Spacing Web Out-of-flatness Criteria.

4.3 I-Shaped Plate Girder Unstiffened Negative Moment

Fig. 33 illustrates the strength based out-of-flatness criterion for the unstiffened web of I-shaped steel plate girders at negative moment. Considering the extreme rate of strength reduction between web slenderness ratios of 124 and 150 and small range of web slenderness no numerical regression was performed to obtain the tolerance as a function of the web slenderness. Conservatively $\frac{D}{150}$ web out-of-flatness was used for the out-of-flatness criteria between web slenderness of 124 and 150. The web slenderness ratio of 124 is the critical web slenderness at which the strength decreases drastically for larger web slenderness until the maximum allowed web slenderness of 150 by AASHTO specifications Considering the minuscule difference of strength for grade 50 and grade 100 steel results, the same criterion is offered for the steel grade 100.

If $\frac{D}{t} \leq 124$ then $\Delta_0 \leq \frac{D}{50}$

If $124 < \frac{D}{t} \leq 150$ then $\Delta_0 \leq \frac{D}{150}$

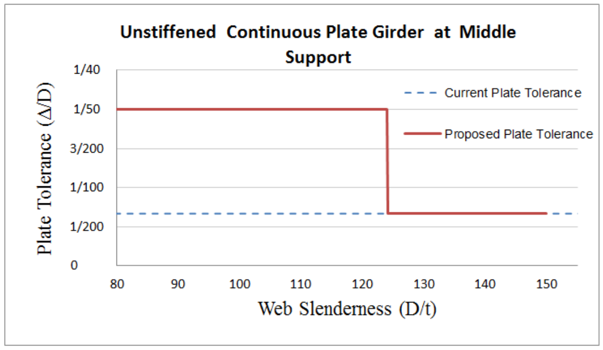

Figure 33: Proposed Strength Based Criteria for Continuous Unstiffened I-Shaped Plate Girder at the Middle Pier.

5. Conclusions

The results of FEA show dependency of first yield moment to web slenderness ratios and out-of-flatness in I-shaped plate girders. There is the critical web slenderness ratio of 124 for unstiffened I-shaped girders which causes the most strength reduction for positive moments and drastic strength reduction for larger slenderness for negative moment. No reverse behavior or critical web slenderness was observed in stiffened I-shaped girders for 1D, 2D, and 3D transverse stiffener spacings. The out-of-flatness tolerance was relaxed when it was strength wise possible. The proposed strength-based web out-of-flatness criteria are provided for I-shaped plate girders. Adopting total body first buckling mode shape as out-of-flatness pattern resulted in more conservative web tolerance than Zhang's proposed web tolerance for unstiffened I-shaped girders at positive moments.

References

AASHTO/LRFD (2017), *AASHTO LRFD Bridge Design Specifications*, 8th edition, American Association of State Highway and Transportation Officials, Washington, D. C.

ANSYS (2013), *Finite Element Program User's Manual*, Version 15.0, ANSYS, Inc., Canonsburg, PA.

AWS D1.5 (2015), *Bridge Welding Code – Steel*, ANSI/AASHTO/AWS D1.5M/D1.5:2015.

Herman, R.S. (2001), "Behavior of Stiffened Compression Flanges of Trapezoidal Box Girder Bridges", *Ph.D. Dissertation*, Department of Civil, Architectural, and Environmental Engineering, University of Texas, Austin, TX.

Korol, R.M. and Thimmhardy, E.G., and Cheung, M.S. (1984), "Field investigation of out-of-plane deviations for steel tub girder bridges", *Can. J. Civ. Eng.*, 11. pp. 377-386.

Rangelov, N. (1992), "A Theoretical Approach to the Limiting of Initial Imperfections in Steel Plates" *Stahlbau*, Vol. 61, pp. 151-156.

Sadovsky, Z. (1978), "A Theoretical Approach to the Problem of the Most Dangerous Initial Deflection Shape in Stability Type Structural Problems" *Aplikace Matematiky*, Vol. 23, pp. 248-266.

Sadovsky, Z. (1996), "Tolerances of Initial Deflections of Steel Plates and Strength of I Cross-section in Compression and Bending" *Journal of Constructional Steel Research*, Vol. 38, No. 3, pp.219-238.

Salmon Charles G., Johnson John E. and Malhas Faris A., (2008), "Steel Structures Design and Behavior" Paper Book, 5th Edition.

Zhang, Yue (2007), "strength-based Plate Tolerances for Steel Bridge Girders." *Ph.D. Dissertation*, Department of Civil, Architectural, and Environmental Engineering, University of Houston, Houston, TX.